Symmetry classification of energy bands in graphene

E. Kogan*
Department of Physics, Bar-Ilan University, Ramat-Gan 52900, Israel

V. U. Nazarov†
Research Center for Applied Sciences, Academia Sinica, Taipei 11529, Taiwan

(Received 31 January 2012; revised manuscript received 22 February 2012; published 14 March 2012; corrected 19 March 2012)

We present the results of the first-principle calculations of the energy bands in graphene and their symmetry classification. The valence bands and four lowest conduction bands are classified according to their symmetry at points Γ and K. Merging of the bands is interpreted in the framework of the group theory.

DOI: 10.1103/PhysRevB.85.115418 PACS number(s): 73.22.Pr

I. INTRODUCTION

Since graphene was first isolated experimentally,[1] it is the focus of attention of both theorists and experimentalists. Obviously our understanding of graphene starts from the knowledge of its energy bands. It is common knowledge that the highest valence (π) band and the lowest lying conduction (π^*) band merge at the Fermi level at point K (the corner of the Brillouin zone). The dispersion law of these two bands (obtained in the tight-binding approximation) is also well known since the seminal paper by Wallace.[2,3] The other bands in graphene were also studied previously, although in a much less detailed way than the above mentioned two. In particular, there were performed first-principle calculations of the band structure of graphene.[4–8]

However, a crucial element in our understanding of the band structure of graphene is still missing, that is the symmetry analysis of the bands. Such analysis (for any periodic crystal Hamiltonian) is most easily performed with the help of elementary group theory.[9,10] The symmetry of crystal is characterized by a point group R. Any operation of this group (save the unit transformation) takes a general wave vector $\mathbf{k}$ into a distinct one. However, for some special choices of $\mathbf{k}$ some of the operations of the crystal symmetry group will take $\mathbf{k}$ into itself rather than into a distinct wave vector. These particular operations are called the group of $\mathbf{k}$; it is a subgroup of the full symmetry group of the crystal. Lines in the Brillouin zone for which the group of the wave vector contains elements other than the unit element are called symmetry lines. At special points in the Brillouin zone the group of the wave vector may be larger than that on symmetry lines which thread it; these are called symmetry points. We may use a state (states) corresponding to such a special wave vector to generate a representation for the group of $\mathbf{k}$.[9,10] (For an arbitrary wave vector, of course, the group of the wave vector is simply E, and the only irreducible representation which may be realized by the states corresponding to such a wave vector is the unit representation.)

We may classify states at a wave vector corresponding to a symmetry point according to the irreducible representation of the group of the wave vector at that point. As the wave vector then moves away from the point, the group of the wave vector becomes smaller and some of the degeneracies will be split. We may determine the irreducible representations into which the original representation will split. Conditions relating the irreducible representations of adjoining points and lines are called compatibility relations and were discussed in Ref. 11. The early classical papers in the field are reprinted in Ref. 12. The energy band calculations are most commonly carried out along symmetry lines in the Brillouin zone.

II. SYMMETRY CLASSIFICATION OF THE ENERGY BANDS

We have calculated the band structure of graphene along the Γ-K-M-Γ line with the code Elk[13] which implements the full potential linearized plane wave method (FP-LAPW)[14] and the local-density approximation (LDA) exchange-correlation (xc) potential. The k-vector grid was unshifted with $64 \times 64 \times 1$ points with all the symmetries applied. The separation d between the periodically repeated in the perpendicular direction graphene layers was chosen at 200 bohr. With this, the elimination of the interlayer interaction has been ensured.

The results of the calculation are presented in Fig. 1. The curves have been found well converged with respect to the further increase of d and they represent the intrinsic nine lowest-lying valence and conduction bands of graphene. While the overall agreement with previous pseudopotential-based band-structure calculations[4–6,15] is found, one important point warrants a special noting: In Ref. 15, the two low-lying (Γ point) bands were attributed to image-potential states. Since, in contrast to Ref. 15, we do not impose an additional image potential, and since LDA for xc potential does not account for the latter,[16] we conclude that the two bands in question are ordinary Kohn-Sham LDA energy bands rather than the image-state bands.

The gray background in Fig. 1 represents the continuous spectrum which is extrapolated in the $d \to \infty$ limit from the quasicontinuous one obtained from the calculations. The edge of the continuum is at approximately 4.6 eV at the Γ point which gives the vacuum level in this calculation. The bands entering continuum (red lines inside the gray background) turn into resonances, that is, the corresponding wave functions leak out from the graphene plane into vacuum. However, this leakage is apparently weak as indicated by the stability of the corresponding bands with respect to the d increase. The studies of the width of the resonances, including those corresponding to the higher bands, will be submitted for publication separately.

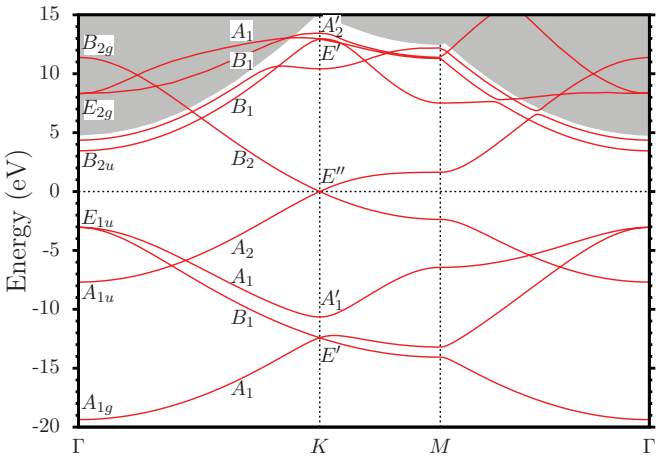

FIG. 1. (Color online) Graphene band structure evaluated with use of the FP-LAPW method. The red-marked lines are well-converged single graphene layer bands, while the gray background corresponds to continuous spectrum.

The symmetry points in graphene are point Γ, the center of the Brillouin zone, points K, which are corners of the Brillouin zone, and points M, which are the centers of the edges of the Brillouin zone. The symmetry lines are Γ-K, Γ-M, and K-M lines. The small group of vector $\mathbf{k}$ at point Γ is D_{6h}. The small group of vector $\mathbf{k}$ at point K is D_{3h}. The small group of vector $\mathbf{k}$ at lines Γ-K is C_{2v}.

The representation of the group D_{6h} we can obtain noticing that

$$D_{6h} = D_6 \times C_i. \tag{1}$$

Thus representation, say A_1 of group D_6, begets two representations of the group D_{6h}: A_{1g} and A_{1u}, where the letter g or u means that the representation is even or odd with respect to inversion respectively. The z axis is always chosen perpendicular to the graphene plane. When considering the Γ-K line, the x axis is chosen in the direction of the line.

The compatibility relations of the groups are obtained by taking into account that irreducible representations of the groups D_{6h} and D_{3h} become reducible when we consider them as the representations of the group C_{2v}. The expansion of these representations with respect to irreducible representations of the group C_{2v} can be easily done using the tables of characters (Tables I and II). Equation

$$a^{(\alpha)} = \frac{1}{g}\sum_G \chi(G)\chi^{(\alpha)}(G) \tag{2}$$

shows how many times a given irreducible representation is contained in a reducible one, All the relevant compatibility relations are presented in Table III.

Now let us come directly to the classification of the energy bands. We assume that the representation realized by the lowest valence band at point Γ is the maximum symmetry representation A_{1g}. From Table III we immediately come to the conclusion that the band at the line Γ-K is characterized by the representation A_1. The representation A_1 is compatible with one-dimensional representation A_1' and two-dimensional representation E' at point K. But because of degeneracy in this point we come to the conclusion that the lowest valence band realizes the representation E' at point K, and the other band, merging with it at point K, at the line Γ-K realizes the representation B_1. Hence the third band, merging with the second one at point K, at line Γ-K realizes the representation A_1. The second and the third band realize at point Γ either the representation E_{1u} or E_{2g}. Assuming that these two bands produce a bonding (that is symmetric) orbital, we come to the conclusion that they realize at point Γ representation E_{1u}. Taking into account that $\sigma_h = IC_2$, we deduce that these valence bands are even with respect to the σ_h operation.

Let us come to two bands which merge at the Fermi level at point K. It is common knowledge that they are antisymmetric with respect to the σ_h operation (see Sec. III). Among the two bands in question the valence band (π band) is characterized at point Γ by the representation A_{1u} (bonding and, hence, symmetric orbital), and the conduction band (π^* band) is characterized at point Γ by the representation B_{2g} (antibonding and, hence, antisymmetric orbital). At the line Γ-K they are characterized by the representations A_2 and B_2, respectively, and at point K they are characterized by the representation E''.[17,18] It was mentioned already in the classical paper[17] that a two-dimensional representation realized by the wave functions at point K means that the dispersion law in the vicinity of this point can be presented by a circular cone. Similar reasoning can be applied to the lowest lying conduction bands. All the results of symmetry classification are presented in Fig. 1.

The most prominent features in the band structure presented in Fig. 1 is the merging of the bands. In Sec. III we will interpret merging of the π and π^* bands at point K and merging of the

TABLE I. Character tables.

D_6	C_{6v}	D_{3h}	E E E	C_2 C_2 σ_h	$2C_3$ $2C_3$ $2C_3$	$2C_6$ $2C_6$ $2S_3$	$3U_2$ $3\sigma_v$ $3U_2$	$3U_2'$ $3\sigma_v'$ $3\sigma_v$
A_1	A_1	A_1'	1	1	1	1	1	1
A_2	A_2	A_2'	1	1	1	1	−1	−1
B_1	B_2	A_1''	1	−1	1	−1	1	−1
B_2	B_1	A_2''	1	−1	1	−1	−1	1
E_2	E_2	E'	2	2	−1	−1	0	0
E_1	E_1	E''	2	−2	−1	1	0	0

TABLE II. Character tables, $\epsilon = e^{2\pi i/3}$.

C_{2v}	E	C_2	σ_v^{xy}	σ_v^{xz}
A_1	1	1	1	1
A_2	1	1	−1	−1
B_1	1	−1	1	−1
B_2	1	−1	−1	1
C_{3v}	E	$2C_3$	$3\sigma_v$	
A_1	1	1	1	
A_2	1	1	−1	
E	2	−1	0	
C_3	E	C_3	C_3^2	
A	1	1	1	
$E; x+iy$	1	ϵ	ϵ^2	
$E; x-iy$	1	ϵ^2	ϵ	

TABLE III. Compatibility relations for the honeycomb lattice (Γ-K line).

C_{2v} Rep	D_{6h}	D_{3h} Compatible with	D_{2h}
A_1	$A_{1g},B_{1u},E_{1u},E_{2g}$	A_1',E'	A_g,B_{1g},B_{2u},B_{3u}
A_2	$A_{1u},B_{1g},E_{1g},E_{2u}$	A_1'',E''	A_u,B_{1u},B_{2g},B_{3g}
B_1	$A_{2g},B_{2u},E_{1u},E_{2g}$	A_2',E'	A_g,B_{1g},B_{2u},B_{3u}
B_2	$A_{2u},B_{2g},E_{1g},E_{2u}$	A_2'',E''	A_u,B_{1u},B_{2g},B_{3g}

σ bands at point Γ using the tight-binding model. In Sec. IV we will interpret merging of the bands at point K exclusively in the framework of the group theory.

III. TIGHT-BINDING HAMILTONIAN + GROUP THEORY

It is interesting to look at the proposed symmetry classification of the bands in general and at their merging in particular from the point of view of the tight-binding model. In isolated form, carbon has six electrons in the orbital configuration $1s^2 2s^2 2p^2$. When arranged in the honeycomb crystal, two electrons remain in the core $1s$ orbital, and are traditionally ignored in band calculations. The remaining four electrons occupy four valence bands; there are also conduction bands, of which a few lowest ones are of interest. The tight-binding Hamiltonian for sp-bonded systems includes four orbitals per atom: s,p_x,p_y,p_z. The Hamiltonian, being symmetric with respect to reflection in the graphene plane, the bands built from the p_z orbitals decouple from those built from s,p_x,p_y orbitals. The former are odd with respect to reflection in the graphene plane, the latter are even. The classification with respect to reflection in the graphene plane is already done, we can talk about C_{6v} and C_{3v} groups instead of D_{6h} and D_{3h}.

A. The π bands

The structure of graphene can be seen as a triangular lattice with a basis of two atoms per unit cell, displaced from each other by any one (fixed) vector connecting two sites of different sublattices, say $\delta=-a(1,0)$. The general Hamiltonian for the π bands is

$$H=-\begin{pmatrix} \sum_{\mathbf{a}} t'(\mathbf{a})e^{i\mathbf{k}\cdot\mathbf{a}} & \sum_{\mathbf{a}} t(\mathbf{a}+\delta)e^{i\mathbf{k}\cdot(\mathbf{a}+\delta)} \\ \sum_{\mathbf{a}} t^*(\mathbf{a}+\delta)e^{-i\mathbf{k}\cdot(\mathbf{a}+\delta)} & \sum_{\mathbf{a}} t'(\mathbf{a})e^{i\mathbf{k}\cdot\mathbf{a}} \end{pmatrix}, \tag{3}$$

where $\mathbf{a}$ is an arbitrary lattice vector, that is a linear combination of $\mathbf{a}_1=\frac{a}{2}(3,\sqrt{3})$, $\mathbf{a}_2=\frac{a}{2}(3,-\sqrt{3})$.

The selection rule for matrix elements gives

$$\sum_{\mathbf{a}} t(\mathbf{a}+\delta)e^{i\mathbf{K}\cdot(\mathbf{a}+\delta)}=0, \tag{4}$$

where $\mathbf{K}$ is a corner of the Brillouin zone. In fact, we are dealing with the product of two functions: $t(\mathbf{a}+\delta)$ realizes the unit representation of the point symmetry group C_3 (the full symmetry group of the intersublattice hopping is C_{3v}, but the restricted symmetry C_3 will be enough to prove the cancellation). As far as the function $e^{i\mathbf{K}\cdot(\mathbf{a}+\delta)}$ is concerned, rotation of the lattice by the angle $2\pi/3$, say anticlockwise, is equivalent to rotation of the vector $\mathbf{K}$ in the opposite direction, that is to substitution of the three equivalent corners of the Brillouin zone: $\mathbf{K}_1\to\mathbf{K}_2\to\mathbf{K}_3\to\mathbf{K}_1$, where $\mathbf{K}_1=(\frac{2\pi}{3a},\frac{2\pi}{3\sqrt{3}a})$, $\mathbf{K}_2=(0,-\frac{4\pi}{3\sqrt{3}a})$, and $\mathbf{K}_3=(-\frac{2\pi}{3a},\frac{2\pi}{3\sqrt{3}a})$. Thus due to the rotation $e^{i\mathbf{K}\cdot(\mathbf{a}+\delta)}$ is multiplied by the factor ϵ^2 and realizes $x-iy$ representation of the group C_3. Because each of the multipliers in Eq. (4) realizes different irreducible representation of the symmetry group, the matrix element is equal to zero. Simply speaking, at a point $\mathbf{K}$ the sublattices become decoupled, and this explains the degeneracy of the electron states in this point (these points) or, in other words, merging of the two branches of the single Brillouin zone.

On the other hand, generally

$$\sum_{\mathbf{a}} t'(\mathbf{a})e^{i\mathbf{K}\cdot\mathbf{a}}\neq 0. \tag{5}$$

To understand this statement consider the maximum symmetry group of the intralattice hopping: C_{6v}. The function $t'(\mathbf{a})$ realizes the A_1 representation of the group. Applying Eq. (2) we see that reducible representation of the group C_{6v}, realized by the two functions $e^{i\mathbf{K}\cdot\mathbf{a}}$ and $e^{i\mathbf{K}'\cdot\mathbf{a}}$, can be decomposed as A_1+B_2.

In addition, the tight-binding model provides us with a simple explanation of why the dispersion law in the vicinity of the merging points is linear, that is why these points are Dirac points. The dispersion law for the Hamiltonian (3) is given by equation

$$F(E,\mathbf{k})=0, \tag{6}$$

where

$$F(E,\mathbf{k})=\begin{vmatrix} E+\sum_{\mathbf{a}} t'(\mathbf{a})e^{i\mathbf{k}\cdot\mathbf{a}} & \sum_{\mathbf{a}} t(\mathbf{a}+\delta)e^{i\mathbf{k}\cdot(\mathbf{a}+\delta)} \\ \sum_{\mathbf{a}} t^*(\mathbf{a}+\delta)e^{-i\mathbf{k}\cdot(\mathbf{a}+\delta)} & E+\sum_{\mathbf{a}} t'(\mathbf{a})e^{i\mathbf{k}\cdot\mathbf{a}} \end{vmatrix}. \tag{7}$$

In mathematics the Dirac points we are dealing with are called conical points of the surface; if the surface is given by Eq. (6), the conditions for the conical points are[19]

$$\frac{\partial F}{\partial E}=0,\quad \frac{\partial F}{\partial \mathbf{k}}=0. \tag{8}$$

Recalling the rule for differentiating of a determinant, we realize that Eq. (4) guarantees that the conditions (8) for $\mathbf{k}=\mathbf{K}$. This explains linearity of the spectrum in the vicinity of the points $\mathbf{K}$($\mathbf{K}$').

B. The σ bands

We will concentrate on the dispersion law of the σ bands along the Γ-K line. Mirror reflection in this line exchanges the graphene sublattices, changes y to $-y$, and does not change the wave vector. It means that the valence bands labeled by A_1 are constructed from sublattice symmetric combinations of s and p_x orbitals and from sublattice antisymmetric combinations of p_y orbitals. The valence band labeled by B_1 is constructed from sublattice antisymmetric combinations of s and p_x orbitals and from sublattice symmetric combinations of p_y orbitals.

We can be more specific speaking about the valence states at points Γ and K. The states with the symmetry A_{1g} and A_1' are the sublattice symmetric combinations of s orbitals.

The states with the symmetry E_{1u} and E' are the (degenerate) sublattice symmetric combinations of p_x and p_y orbitals.

Looking at the conduction bands we realize that the two bands which merge at point Γ with the symmetry E_{2g} are probably of the same nature as the two valence bands which merge at point Γ with the symmetry E_{1u}, and the states with the symmetry E_{2g} are the (degenerate) sublattice antisymmetric combinations of p_x and p_y orbitals. (In the language of quantum chemistry sublattice symmetric and antisymmetric combinations are bonding and antibonding orbitals, respectively.)

IV. QUASI-FREE ELECTRONS + GROUP THEORY

If we consider separately σ and π states we can ignore the third dimension and treat graphene as purely two dimensional. The Hamiltonian of the electrons is

$$H = H_0 + V, \tag{9}$$

where H_0 is the Hamiltonian of the free electrons and V is the crystalline potential. The following reasoning uses the extended Brillouin zone scheme[20] and is the application of group theory to quantum mechanics.[21]

All the eigenstates of the Hamiltonian H_0 with the same $|\mathbf{k}|$ are degenerate. The potential V having lower symmetry partially (nearly completely) removes the degeneracy. To find the maximum splitting we should find among the continuum of the vectors with the given value of $|\mathbf{k}|$ those which realize an irreducible representation of this or that subgroup of the space group of the crystal. For arbitrary value of $|\mathbf{k}|$ each state is symmetric only with respect to the subgroup of translations and realizes a one-dimensional representation of this subgroup.

However, the states with the wave vector $\mathbf{K}+\mathbf{b}$, where $\mathbf{b}$ is an arbitrary vector of the inverse lattice (corners of the Brillouin zones) have higher symmetry. They realize a representation (infinite dimensional) of the group which includes in addition to translations the point group C_{3v}. We will expand this representation into the irreducible ones in two stages.

First we will divide all the vectors $\mathbf{K}+\mathbf{b}$ into the sets such that elements of a given set are connected with each other by the operations of the group C_{3v}. Such sets turn out to be triplets. For example, the states with the wave vectors $\mathbf{K}_1,\mathbf{K}_1-\mathbf{b}_1,\mathbf{K}_1-\mathbf{b}_1-\mathbf{b}_2$, where $\mathbf{b}_1=\frac{2\pi}{3a}(1,\sqrt{3})$ and $\mathbf{b}_2=\frac{2\pi}{3a}(1,-\sqrt{3})$ are the elementary reciprocal-lattice vectors. Another example is the states having wave vectors $\mathbf{K}_1-\mathbf{b}_2,\mathbf{K}_1+\mathbf{b}_2,\mathbf{K}_1-2\mathbf{b}_1-\mathbf{b}_2$. Still another example is two triplets having the same energy: $\mathbf{K}_1-2\mathbf{b}_1-2\mathbf{b},\mathbf{K}_1+\mathbf{b}_1,\mathbf{K}_1-\mathbf{b}_1+\mathbf{b}_2$ and $\mathbf{K}_1-\mathbf{b}_1-2\mathbf{b}_2,\mathbf{K}_1-2\mathbf{b}_1,\mathbf{K}_1+\mathbf{b}_1+\mathbf{b}_2$.

At the second stage, applying Eq. (2) we decompose the reducible representation R of the symmetry group C_{3v}, generated by a triplet into the irreducible representations. The triplet generates natural representation of the group C_{3v} (Table IV).[22] Applying Eq. (2) we obtain

$$R = A_1 + E. \tag{10}$$

It should be noted that the result does not depend on V being in any sense small.[21]

TABLE IV. Characters of natural representation.

C_{3v}	E	$2C_3$	$3\sigma_v$
R	3	0	1

Recalling the symmetry of the states relative to reflection in the plane of graphene, Eq. (10) can be rewritten as

$$R = A_1' + E' \tag{11}$$

for σ states, and as

$$R = A_2'' + E'' \tag{12}$$

for π states.

A picture that emerges becomes clear in the extended Brillouin zone scheme, where the Brillouin zones fill the whole plane. Each Brillouin zone being a hexagon, three zones meet at their corners; two of them merge.

To find the dispersion law in the vicinity of the merging point we may consider a reduced Hamiltonian,

$$H = \begin{pmatrix} H_{11} & H_{12} \\ H_{21} & H_{22} \end{pmatrix}, \tag{13}$$

where each element is a linear function of k_x,k_y ($\mathbf{k}$ is the deviation of the wave vector from the merging point), and we have shifted the energy axis, such that the energy in the merging point is now zero. The dispersion law for the Hamiltonian (13) is given by equation

$$E = c_i k_i \pm \sqrt{d_{ij}k_i k_j}, \tag{14}$$

describing two cones, which is a general situation for levels crossing.[23] However, in the case considered, we can be more specific about these cones. Because any vector in the k_x,k_y plane compatible with the symmetry C_{3v} is identically equal to zero, and any tensor of rank two compatible with the symmetry is proportional to the unity tensor, the dispersion law is just

$$E \sim \pm|\mathbf{k}|, \tag{15}$$

and the cones are circular, with the axis perpendicular to the k_x,k_y plane.

The important role played by discrete symmetries in protecting a k-linear dispersion in graphene was pointed out in Ref. 24. Reference 25 was an important precedent in applying group theory methods to graphene. The appearance of massless Dirac fermions under conditions of hexagonal symmetry was considered in Ref. 26. Group theory was used to derive an invariant expansion of the Hamiltonian for electron states near the K points of the graphene Brillouin zone in Ref. 27. The influence of stress on the bands merging was analyzed in Refs. 28 and 29. The influence of spin-orbit interactions on the band structure of graphene was studied in Ref. 30.

ACKNOWLEDGMENTS

The work was finalized during one of the authors (E.K.) visit to DIPC, San Sebastian. The authors are grateful to V. Silkin for very useful discussion. The other author (V.U.N.) acknowledges partial support from National Science Council, Taiwan, Grant No. 100-2112-M-001-025-MY3.

---

*eugene.kogan@biu.ac.il

†nazarov@gate.sinica.edu.tw

[1] K. S. Novoselov, A. K. Geim, S. V. Morozov, D. Jiang, Y. Zhang, S. V. Dubonos, I. V. Grigorieva, and A. A. Firsov, Science **306**, 5696 (2004).

[2] P. R. Wallace, Phys. Rev. **71**, 622 (1947).

[3] A. H. Castro Neto, F. Guinea, N. M. R. Peres, K. S. Novoselov, and A. K. Geim, Rev. Mod. Phys. **81**, 109 (2009).

[4] S. Latil and L. Henrard, Phys. Rev. Lett. **97**, 036803 (2006).

[5] T. O. Wehling, I. Grigorenko, A. I. Lichtenstein, and A. V. Balatsky, Phys. Rev. Lett. **101**, 216803 (2008).

[6] P. E. Trevisanutto, C. Giorgetti, L. Reining, M. Ladisa, and V. Olevano, Phys. Rev. Lett. **101**, 226405 (2008).

[7] V. M. Silkin, J. Zhao, F. Guinea, E. V. Chulkov, P. M. Echenique, and H. Petek, Phys. Rev. B **80**, 121408 (2009).

[8] T. Suzuki and Y. Yokomizo, Physica E **42**, 2820 (2010).

[9] C. Kittel, *Quantum Theory of Solids* (John Wiley, New York, 1963).

[10] W. A. Harrison, *Solid State Theory* (McGraw Hill, New York, 1970).

[11] L. P. Bouckaert, R. Smoluchowski, and E. Wigner, Phys. Rev. **50**, 58 (1936).

[12] R. S. Knox and S. Gold, *Symmmetry in the Solid State* (W. A. Benjamin, New York, 1964).

[13] [http://elk.sourceforge.net].

[14] D. H. Singh, *Planewaves, Pseudopotentials, and the LAPW Method* (Kluwer, Boston, MA, 1994).

[15] V. M. Silkin, J. Zhao, F. Guinea, E. V. Chulkov, P. M. Echenique, and H. Petek, Phys. Rev. B **80**, 121408 (2009).

[16] N. D. Lang and W. Kohn, Phys. Rev. B **1**, 4555 (1970).

[17] J. C. Slonczewski and P. R. Weiss, Phys. Rev. **109**, 272 (1958).

[18] C. Thomsen, S. Reich, and J. Maultzsch, *Carbon Nanotubes: Basic Concepts and Physical Properties* (Wiley, New York, 2004).

[19] E. Goursat, *Course D'Analyse Mathematique* (Gauthier-Villars, Paris, 1902-1913) [cited by Russian translation: *Kurs Matematicheskogo Analisa* (Moskow, 1933), Vol. I, Part 1, p. 100].

[20] O. Madelung, *Introduction to Solid-State Theory* (Springer, Berlin, 1996).

[21] V. Heine, *Group Theory in Quantum Mechanics* (Pergamon, New York, 1970).

[22] K. F. Riley, M. P. Hobson, and S. J. Bence, *Mathematical Methods for Physics and Engineering*, 3rd ed. (Cambridge University Press, Cambridge, 2006).

[23] L. D. Landau and E. M. Lifshitz, *Quantum Mechanics* (Pergamon, New York, 1991).

[24] J. L. Manes, F. Guinea, and M. A. H. Vozmediano, Phys. Rev. B **75**, 155424 (2007); J. L. Manes, e-print arXiv:1109.2581v2.

[25] L. M. Malard, M. H. D. Guimaraes, D. L. Mafra, M. S. C. Mazzoni, and A. Jorio, Phys. Rev. B **79**, 125426 (2009).

[26] C.-H. Park and S. G. Louie, Nano Lett. **9**, 1793 (2009).

[27] R. Winkler and U. Zulicke, Phys. Rev. B **82**, 245313 (2010).

[28] V. M. Pereira, A. H. Castro Neto, and N. M. R. Peres, Phys. Rev. B **80**, 045401 (2009).

[29] R. M. Ribeiro, V. M. Pereira, N. M. R. Peres, P. R. Briddon, and A. H. Castro Neto, New J. Phys. **11**, 115002 (2009).

[30] H. Min, J. E. Hill, N. A. Sinitsyn, B. R. Sahu, L. Kleinman, and A. H. MacDonald, Phys. Rev. B **74**, 165310 (2006).